

Chaos and hyperchaos of geodesic flows on curved manifolds corresponding to mechanically coupled rotators: Examples and numerical study

S.P. Kuznetsov

October 19, 2018

*Udmurt State University, Universitetskaya 1, Izhevsk, 426034,
Russian Federation*

*Kotel'nikov's Institute of Radio-Engineering and Electronics of RAS,
Saratov Branch, Zelenaya 38, Saratov, 410019, Russian Federation*

Abstract

A system of N rotators is investigated with a constraint given by a condition of vanishing sum of the cosines of the rotation angles. Equations of the dynamics are formulated and results of numerical simulation for the cases $N=3, 4$, and 5 are presented relating to the geodesic flows on a two-dimensional, three-dimensional, and four-dimensional manifold, respectively, in a compact region (due to the periodicity of the configuration space in angular variables). It is shown that a system of three rotators demonstrates chaos, characterized by one positive Lyapunov exponent, and for systems of four and five elements there are, respectively, two and three positive exponents (“hyperchaos”). An algorithm has been implemented that allows calculating the sectional curvature of a manifold in the course of numerical simulation of the dynamics at points of a trajectory. In the case of $N=3$, curvature of the two-dimensional manifold is negative (except for a finite number of points where it is zero), and Anosov’s geodesic flow is realized. For $N=4$ and 5 , the computations show that the condition of negative sectional curvature is not fulfilled. Also the methodology is explained and applied for testing hyperbolicity based on numerical analysis of the angles between the subspaces of small perturbation vectors; in the case of $N=3$, the hyperbolicity is confirmed, and for $N=4$ and 5 the hyperbolicity does not take place.

Geodesic flows represent a special class of dynamical systems, the phase space of which is the set of points of a certain manifold together with the velocity vectors at these points [1, 2]. Motion takes place along geodesic lines, with preservation of the velocity component in the direction of the geodesic. This is a natural generalization of the free motion of a material point by inertia in Euclidean space to the case of motion on a curved surface or in a multidimensional space with curvature.

Geodesic flows on compact manifolds of negative curvature serve as a classic example of deterministic chaos, which belongs to the category of hyperbolic dynamics possessing the property of roughness or structural stability. Early examples go back to Hadamard [3], but the valuable development of the corresponding part of the theory of dynamical systems progressed in 1960s-1970s due to seminal work of Anosov and other researchers [4, 5, 6, 7].

Natural area of application of the geodesic flows with nontrivial dynamics relates to mechanical systems that perform motion under conditions of conservation of mechanical energy with imposed holonomic constraints being defined by algebraic relations between the coordinates. The constraint equations determine shape of the manifold as an object embedded in the ambient space, and the metric on the manifold is naturally determined by the quadratic form of the expression for kinetic energy through generalized velocities.

Fig. 1a shows a mechanism built from three two-link cranks, which was proposed as an example of a system with configuration space being a nontrivial manifold by Thurston and Weeks [8]. It can be interpreted as a system of three rotators with a constraint defined by certain algebraic relation between the angular coordinates. Hunt and MacKay showed that the free motion of this mechanism with proper selection of parameters provides a feasible example of the Anosov flow on compact two-dimensional manifold of negative curvature [9]. The special case, when the constraint equation is simplified (in certain asymptotics in parameters) and reduces to a condition of vanishing sum of cosines of the three angles of revolution of the rotators about their fixed axes, was discussed in detail in [10, 11]. The configuration space in this case is a two-dimensional curved surface, known as the Schwarz P-surface [12]. Also generalizations were considered that imply replacement of the algebraic constraint equations by a potential interaction of the rotators of such kind that the minimum of the potential function takes place just on the Schwarz surface [13, 14, 15]. Introduction of dissipation and feedbacks into the system was discussed, which allowed realizing chaotic self-oscillations generated by a hyperbolic structurally stable attractor. On this base an electronic device reproducing the Anosov dynamics was designed, which is a generator of rough chaos with characteristics attractive for applications [14, 15].

It seems natural to turn to generalizations consisting in considering systems based on a different number of rotators.

A case of two rotators with constraint implemented by means of a hinge mechanism appears to be not interesting in respect to its dynamics, as it is rather trivial since the configuration space degenerates into a set of intersecting straight lines on the plane of two angular variables. However, by replacing the mechanical constraint by interaction of the rotators by potential forces, some nontrivial motions such as wandering on a two-dimensional lattice in the plane of angular variables can be observed [16], similar to those orbits on the phase plane of non-autonomous systems, which provide the so-called Zaslavsky stochastic web [17].

The subject of this article is consideration of the systems constituted by a larger number of rotators N (concretely, the cases of $N=3, 4, 5$ will be dis-

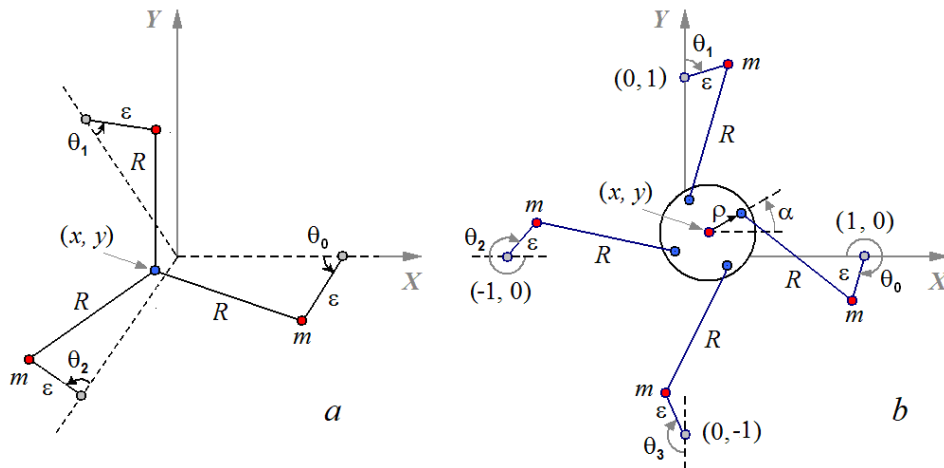


Figure 1: Hinge mechanisms based on rotators, whose angles of revolution about fixed axes are given by $\theta_i(t)$, with imposed holonomic constraint, which in the limiting case $\varepsilon \ll R = 1$ reduces to the equation $\sum_{i=0}^{N-1} \cos \theta_i = 0$, where $N=3$ (a) or 4 (b).

cussed), where the angles of rotation $\theta_0, \theta_1, \dots, \theta_{N-1}$ satisfy the constraint equation

$$\sum_{i=0}^{N-1} \cos \theta_i = 0. \quad (1)$$

In particular, for $N=4$, the corresponding situation can be implemented in the hinge mechanism shown in Fig. 1b, under assumption of certain asymptotics in parameters (see Appendix).

In Section 1, equations are formulated for a system of N rotators with constraint defined by the condition that sum of the cosines of the angles of rotation equals zero. Two forms of equations are presented, one in the ambient space with the imposed constraint condition, which is convenient when numerically integrating the equations and processing the data, and second is an equivalent formulation using the standard notation of theory of Riemannian manifolds [18], which allows establishing and discussing the relationship with the context of Anosov's theory. Section 2 presents and compares the numerical results of analysis of the dynamics for $N=3$, which is the case of Anosov's dynamics corresponding to chaos with one positive Lyapunov exponent, $N=4$ that is hyperchaotic dynamics with two positive Lyapunov exponents on a three-dimensional curved manifold, and $N=5$ that is hyperchaotic dynamics on a four-dimensional manifold with three positive Lyapunov exponents. Section 3 introduces algorithm for calculating the curvature at the points of the trajectory, which was tested by comparing with the analytical formula for the case $N=3$, where the curvature is negative except for a finite number of points on the manifold, and

dynamics is Anosov's. For the cases $N=4$ and 5 it is shown that the condition of negative sectional curvature is not fulfilled: while moving along typical trajectories, positive values of sectional curvatures also occur, so that the geodesic flows under consideration cannot be classified as Anosov's basing on the curvature. Section 4 discusses the technique and presents the results of testing the hyperbolicity of the observed dynamics on a base of analysis of statistics for the intersection angles for subspaces of vectors of small perturbations. It is shown numerically that in the case of $N=3$ the hyperbolicity is confirmed, and in the cases $N=4$ and 5 there is no hyperbolicity. In conclusion, we discuss possible prospects for development of the outlined approaches to analysis of chaotic dynamics, both for geodetic flows and for some other types of nonlinear dynamical systems implementing similar dynamics.

1 Basic equations

Consider a system composed of $N > 2$ rotators characterized by time-dependent instantaneous angles of rotation θ_i , $i = 0, 1, 2, \dots, N - 1$, each of which possesses unit moment of inertia, assuming that the kinetic energy is given by

$$T = \frac{1}{2} \sum_{i=0}^{N-1} \dot{\theta}_i^2, \quad (2)$$

and impose the constraint

$$F(\theta_0, \theta_1, \dots, \theta_{N-1}) = \sum_{i=0}^{N-1} \cos \theta_i = 0. \quad (3)$$

For $N=3$ and 4 it can be implemented by means of the hinge mechanisms mentioned in the Introduction.

The Lagrange equations of motion of the system are

$$\ddot{\theta}_i = \Lambda \partial F / \partial \theta_i = -\Lambda \sin \theta_i, \quad i = 0, 1, N - 1, \quad (4)$$

where the factor Λ is to be determined taking into account the algebraic mechanical constraint condition (3) that is complementary to the differential equations.

Differentiating the constraint equation twice

$$\sum_{i=0}^{N-1} \ddot{\theta}_i \sin \theta_i + \sum_{i=0}^{N-1} \dot{\theta}_i^2 \cos \theta_i = 0, \quad (5)$$

and substituting here the expressions for the second derivatives from (4), we obtain an explicit formula for the factor Λ

$$\Lambda = \frac{\sum_{i=0}^{N-1} \dot{\theta}_i^2 \cos \theta_i}{\sum_{i=0}^{N-1} \sin^2 \theta_i}. \quad (6)$$

Thus, we arrive at the following closed set of equations

$$\ddot{\theta}_i = -\frac{\sum_{j=0}^{N-1} \dot{\theta}_j^2 \cos \theta_j}{\sum_{j=0}^{N-1} \sin^2 \theta_j} \sin \theta_i, \quad i = 0, 1, \dots, N-1, \quad (7)$$

or, equivalently,

$$\dot{\theta}_i = u_i, \quad \dot{u}_i = -\frac{\sum_{j=0}^{N-1} u_j^2 \cos \theta_j}{\sum_{j=0}^{N-1} \sin^2 \theta_j} \sin \theta_i, \quad i = 0, 1, \dots, N-1. \quad (8)$$

The constraint condition (3) and the relation obtained by its differentiation correspond to two first integrals of this system, which formally has order $2N$. The initial conditions must be selected with restriction that these first integrals have the required values, namely,

$$\sum_{i=0}^{N-1} \cos \theta_i = 0 \quad (9)$$

and

$$\sum_{i=0}^{N-1} u_i \sin \theta_i = 0. \quad (10)$$

Dynamics of the system (8) can be interpreted as motion of a particle on manifold of dimension $N-1$ defined by equation (3), along geodesic lines of the metric provided by quadratic form corresponding to the expression for the kinetic energy, namely

$$ds^2 = \sum_{i=0}^{N-1} d\theta_i^2, \quad (11)$$

with the condition $\sum_{i=0}^{N-1} \sin \theta_i d\theta_i = 0$ arising due to the constraint equation. Since the quantities θ_i have the meaning of angular coordinates, they can be considered as related to intervals $(-\pi, \pi)$, and the dynamics may be regarded as occurring in a compact domain.

As evident from the equations, the motions that differ only by the value of the kinetic energy are identical up to a time scale and a value of velocity along the geodesic. In this regard, all the specific data will be given hereafter only for the case of a unit absolute value of velocity, which corresponds to the energy $T = \frac{1}{2}$.

The dynamics of the systems for the number of rotators 3, 4, and 5 are illustrated in Fig. 2 by graphs of angular velocities as functions of time obtained from numerical integrating equations (8) by means of the Runge – Kutta method. As seen from the figure, in all cases the behavior looks chaotic: the dependences demonstrate obvious irregularity and absence of visible repetition of forms. The chaotic nature of the dynamics is also confirmed by the type

of power spectra shown in Fig.3. The spectra were obtained by processing the time series for angular velocity of one of the rotators using data of numerical integration of the equations, with application of the method of statistical evaluation of the spectral density developed for random processes [19, 20]. For this, the time series is divided into sections of certain duration, significantly exceeding the characteristic time scale of the signal, with multiplying data for each segment by the “window” function (to improve the quality of spectral analysis due to removing, as far as possible, the effect of signal mismatch at the edges of the partition intervals). Next, the Fourier transform is performed for each segment, and the squares of the amplitudes of the spectral components are averaged over a set of the segments. It can be seen from the figure that in each of the cases considered the spectra are continuous, like for random processes; there are no expressed discrete components. The chaotic nature of the dynamics is also confirmed by analysis of Lyapunov exponents in the next Section.

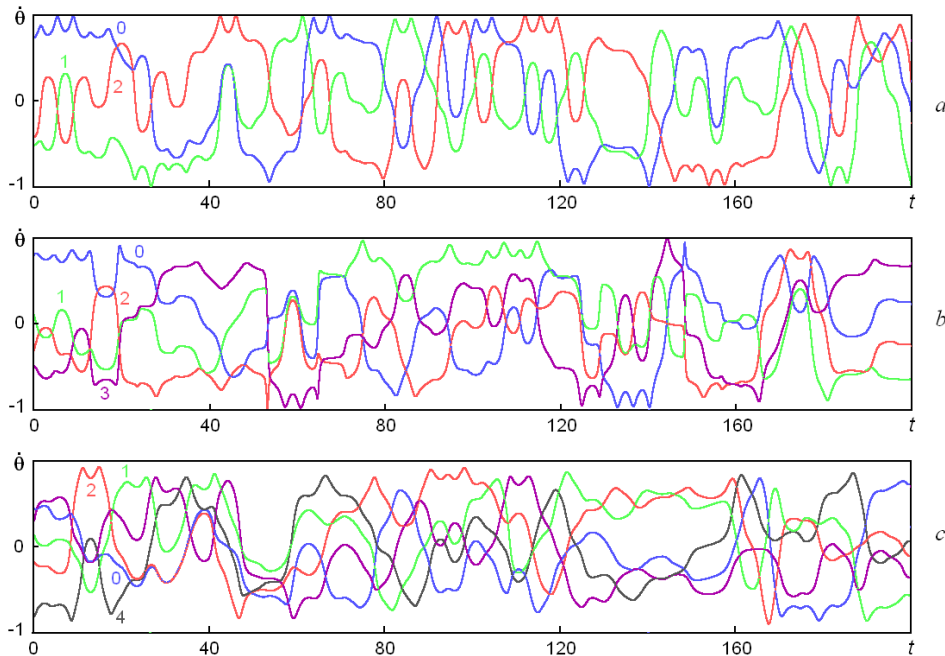


Figure 2: Waveforms of the angular velocities for the system (8) in the cases $N=3$ (a), $N=4$ (b) and $N=5$ (c) obtained numerically for motions with unit velocity in the direction of the geodesics.

The above dynamical equations (7) or (8) can be rewritten using notation adopted in the theory of Riemannian manifolds. For this, we express angular coordinate and velocity of one of the rotators, say, θ_0 and u_0 , in terms of coordinates and velocities of the other rotators, while the set of their angular velocities $(u_1, u_2, \dots, u_{N-1})$ is assumed to be components of a contravariant vec-

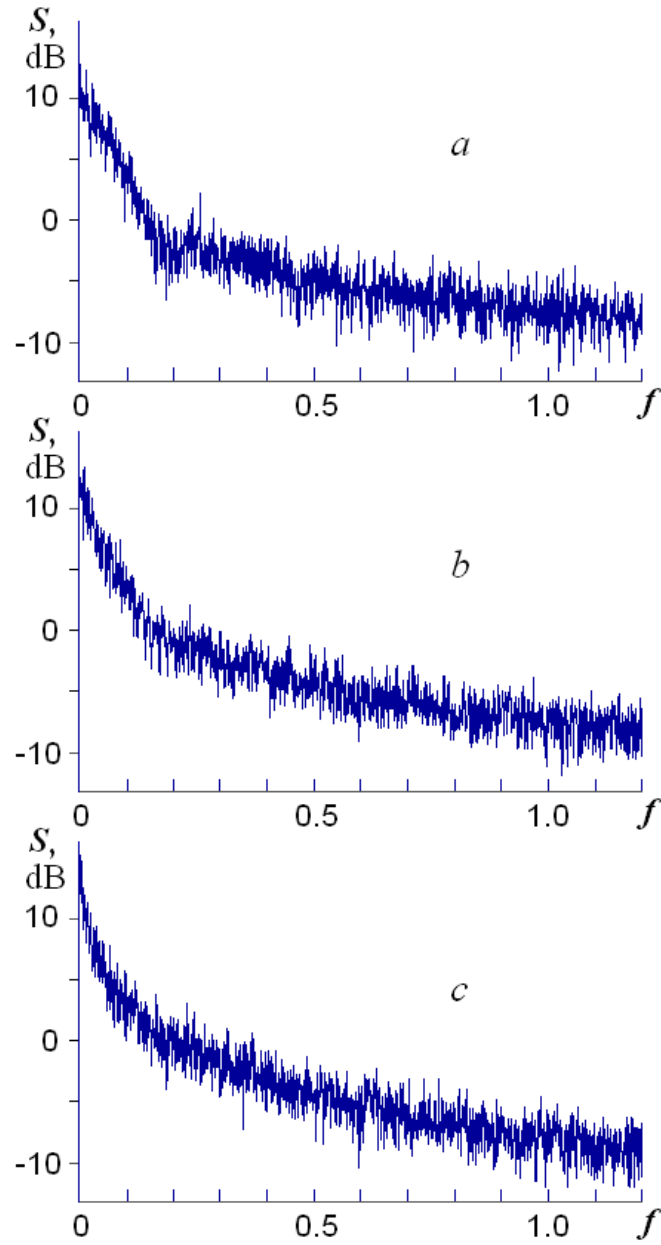


Figure 3: Spectral power density plots of signal given by angular velocity of one of the rotators as obtained from processing data of numerical simulation of the system (8) for the cases $N=3$ (a), $N=4$ (b) and $N=5$ (c) for the motion with unit velocity along the geodesics.

tor u^α , $\alpha = 1, 2, \dots, N-1$. Substituting the result into the formula for kinetic energy, we have

$$T = \frac{1}{2} g_{\alpha\beta} u^\alpha u^\beta, \quad (12)$$

where the Greek indices run from 1 to $N-1$, and summation is assumed over repeating superscripts and subscripts. Components of the metric tensor $g_{\alpha\beta}$ are given by the relations

$$g_{\alpha\beta} = \delta_{\alpha\beta} + \frac{\sin \theta_\alpha \sin \theta_\beta}{1 - \left(\sum_{\gamma=1}^{N-1} \cos \theta_\gamma \right)^2}. \quad (13)$$

The equation of motion then takes the form known for geodesic flows [1, 2, 5, 6], namely,

$$\dot{u}^\alpha + \Gamma_{\beta\gamma}^\alpha u^\beta u^\gamma = 0, \quad (14)$$

where the Christoffel symbols $\Gamma_{\beta\gamma}^\alpha$ are involved, which have expressions through the components of the metric tensor given by standard formulas, and in our particular case they are

$$\Gamma_{\beta\gamma}^\alpha = \frac{\delta_{\beta\gamma} \cos \theta_\beta - \sin \theta_\beta \sin \theta_\gamma \sum_{\nu=1}^{N-1} \cos \theta_\nu \left[1 - \left(\sum_{\nu=1}^{N-1} \cos \theta_\nu \right)^2 \right]^{-1}}{1 + \sum_{\nu=1}^{N-1} \sin^2 \theta_\nu - \left(\sum_{\nu=1}^{N-1} \cos \theta_\nu \right)^2} \sin \theta_\alpha. \quad (15)$$

Among formulas of Riemannian geometry, it is useful to keep in mind the relation that allows tracing components of a vector p^α in the course of parallel transport along a geodesic:

$$\dot{p}^\alpha + \Gamma_{\beta\gamma}^\alpha u^\beta p^\gamma = 0. \quad (16)$$

The above relations, where θ_0 and u^0 play the distinguished role, correspond to a particular choice of one of N charts constituting the atlas of the manifold under consideration. For other charts of the atlas the formulas are similar and are obtained by cyclic permutations of the indices.

2 Lyapunov exponents

Formally, the dimension of the phase space of the system (8) is $2N$. Respectively, there are $2N$ Lyapunov exponents characterizing the behavior of disturbances near a reference trajectory. However, among them, there are two nonphysical zero exponents, which correspond to perturbations of the integrals of motion responsible for the imposed constraint, namely, the perturbations violating the constraint equations. They should be excluded; therefore, the total number of significant Lyapunov exponents is $2N-2$. Due to the conservative nature of the system and symmetry with respect to the time reversal, the presence of each positive exponent implies the presence of another negative one, with equal absolute value. The spectrum of relevant Lyapunov exponents also contains

necessarily two zero exponents, one of which appears because of the autonomous nature of the system being responsible for a perturbation directed tangentially to the phase trajectory, and the second is associated with a perturbation produced by an energy shift.

From the above, it follows that to obtain the full spectrum of Lyapunov exponents it is sufficient to calculate the largest $N - 2$ exponents. This can be done within the framework of computational procedure that implements the joint solution of the dynamical equations (8) together with a set of $N - 2$ equations in variations [21, 22, 23, 24, 25]. The equations in variations are obtained by substituting in (8) dynamic variables with added perturbations: $\theta_i \rightarrow \theta_i + \tilde{\theta}_i$, $u_i \rightarrow u_i + \tilde{u}_i$, and by linearization retaining the first-order terms for small perturbations:

$$\begin{cases} \dot{\tilde{\theta}}_i = \tilde{u}_i, \\ \dot{\tilde{u}}_i = -\frac{\sum_{j=0}^{N-1} (2u_j \tilde{u}_j \cos \theta_j - u_j^2 \tilde{\theta}_j \sin \theta_j)}{\sum_{j=0}^{N-1} \sin^2 \theta_j} \sin \theta_i - \left(\frac{\sum_{j=0}^{N-1} u_j^2 \cos \theta_j}{\sum_{j=0}^{N-1} \sin^2 \theta_j} \right) \tilde{\theta}_i \cos \theta_i \\ + \frac{\left(\sum_{j=0}^{N-1} u_j^2 \cos \theta_j \right)}{\left(\sum_{j=0}^{N-1} \sin^2 \theta_j \right)^2} \sum_{j=0}^{N-1} \tilde{\theta}_j \sin 2\theta_j, \quad i = 0, 1, \dots, N - 1. \end{cases} \quad (17)$$

In the framework of the computational procedure [21, 22, 23, 24, 25], at each step of integrating the differential equations, the obtained $N - 2$ perturbation vectors $\xi = (\tilde{\theta}_0, \dots, \tilde{\theta}_{N-1}, \tilde{u}_0, \dots, \tilde{u}_{N-1})$ are subjected to Gram - Schmidt orthogonalization and normalization:

$$\begin{aligned} \mathbf{x}_1 &= \xi^{(1)}(t), \\ \tilde{\mathbf{x}}^{(1)}(t) &= \mathbf{x}_1 / \langle \mathbf{x}_1, \mathbf{x}_1 \rangle, \\ \mathbf{x}_2 &= \xi^{(2)}(t) - \langle \xi^{(2)}(t), \tilde{\mathbf{x}}^{(1)}(t) \rangle \tilde{\mathbf{x}}^{(1)}(t), \\ \tilde{\mathbf{x}}^{(2)}(t) &= \mathbf{x}_2 / \langle \mathbf{x}_2, \mathbf{x}_2 \rangle, \\ \mathbf{x}_3 &= \xi^{(3)}(t) - \langle \xi^{(3)}(t), \tilde{\mathbf{x}}^{(1)}(t) \rangle \tilde{\mathbf{x}}^{(1)}(t) - \langle \xi^{(3)}(t), \tilde{\mathbf{x}}^{(2)}(t) \rangle \tilde{\mathbf{x}}^{(2)}(t), \\ \tilde{\mathbf{x}}^{(3)}(t) &= \mathbf{x}_3 / \langle \mathbf{x}_3, \mathbf{x}_3 \rangle, \\ &\dots \end{aligned} \quad (18)$$

where the angle brackets denote the scalar product. In our case, it is convenient to use the definition of the scalar product involving only the coordinate components of the vectors, namely, $\langle \xi^{(s)}, \xi^{(r)} \rangle = \sum_{j=0}^{N-1} \tilde{\theta}_j^{(s)} \tilde{\theta}_j^{(r)}$. (This will be useful and adequate also in the calculating the curvatures, as described in the next Section.) A numerical estimate of the Lyapunov exponents is given by cumulative sums of logarithms of norms $\sqrt{\langle \mathbf{x}_i, \mathbf{x}_i \rangle}$ divided by the observation time.

Since there is no characteristic time scale in the system, the non-zero Lyapunov exponents characterizing the exponential growth and decrease of perturbations per unit of time are directly proportional to the velocity, that is, to the

square root of kinetic energy. In this regard, all results are given here only for the case of unit velocities along the geodesics.

Numerical calculations performed for the cases $N=3$, 4, and 5 give the following values for the Lyapunov exponents.

$N=3$:

$$\lambda_1 = 0.500, \lambda_2 = 0, \lambda_3 = 0, \lambda_4 = -0.500.$$

$N=4$:

$$\lambda_1 = 0.385, \lambda_2 = 0.230, \lambda_3 = 0, \lambda_4 = 0, \lambda_5 = -0.230, \lambda_6 = -0.385.$$

$N=5$:

$$\lambda_1 = 0.298, \lambda_2 = 0.227, \lambda_3 = 0.121, \lambda_4 = 0, \lambda_5 = 0,$$

$$\lambda_6 = -0.121, \lambda_7 = -0.227, \lambda_8 = -0.298.$$

As seen, in all three cases there are positive Lyapunov exponents that indicate chaotic nature of the dynamics.

In the first case, $N=3$, when the motion takes place on a two-dimensional manifold representing the Schwarz surface, there is one positive Lyapunov exponent. In the second case, $N=4$, the motion takes place on a three-dimensional curved manifold being characterized by two positive Lyapunov exponents. Finally, in the case $N=5$, we have the motion on a four-dimensional curved manifold, and there are three positive exponents. Chaotic behavior with a number of positive Lyapunov exponents more than one, in the literature is called hyperchaos [26, 27].

3 Curvature

We now turn to consideration of a numerical method for evaluation of the curvature of manifolds at points visited by trajectories. A complete description of the local curvature of manifolds is given by the Riemann tensor [18]. However, bearing in mind the content of the Anosov theory, it is natural to turn to an alternative method for quantifying the curvature, namely, in terms of sectional curvatures [5, 6]. According to Anosov, the hyperbolic nature of the chaotic dynamics of a geodesic flow and, accordingly, its structural stability (roughness), is guaranteed if the sectional curvature is everywhere negative.

Let us consider motion with a unit absolute velocity along a certain reference trajectory representative for our geodesic flow, as well as motions obtained by infinitesimal displacements in the directions orthogonal to the geodesic with the same absolute velocity. Moving along the reference trajectory in the process of numerical integrating the equations (8), we simultaneously integrate a set of equations in variations (17), like in the procedure of calculating the Lyapunov exponents. For each point $A = (\theta_0, \theta_1, \dots, \theta_{N-1})$, visited when performing the numerical integration of the equations, we define an orthonormal basis of N

vectors $\mathbf{p}^{(0)}, \dots, \mathbf{p}^{(N-1)}$ in the tangent space. It is assumed that the vector \mathbf{p}_0 is directed along the reference trajectory, i. e. $\mathbf{p}^{(0)} = (u_0, u_1, \dots, u_{N-1})$, and the rest ones are specified as the coordinate components of the Lyapunov vectors at A , subjected to orthogonalization and normalization, namely, $\mathbf{p}^{(i)} = (\tilde{\theta}_0^{(i)}, \dots, \tilde{\theta}_{N-1}^{(i)})$, $i = 1, \dots, N - 2$.

Further, applying the same difference scheme as used for integrating the differential equations (8) and the variational equations (17), the components of the reference basis vectors are calculated by their parallel transfer along the reference geodesic at points shifted from the initial position by one time step Δt back and forth. This is done by numerical solving the equations

$$\dot{p}_i^{(k)} = - \frac{\sum_{j=0}^{N-1} p_j^{(k)} u_j \cos \theta_j}{\sum_{j=0}^{N-1} \sin^2 \theta_j} \sin \theta_i, \quad i = 0, 1, \dots, N - 1. \quad (19)$$

As can be shown, these equations correspond exactly to the relation (16) in the notation of Riemannian geometry.

Finally, the coefficients $c^{(k)}$ for the expansion in the basis $\mathbf{p}^{(1)}, \dots, \mathbf{p}^{(N-1)}$ are calculated for Lyapunov vectors at the points $t \pm \Delta t$. These coefficients must satisfy the following equation [6], p.136:

$$\frac{d^2 c_i^{(k)}}{dt^2} + \sum_{k=1}^{N-1} K_{ij}(t) c_j^{(k)} = 0, \quad (20)$$

where the symmetric matrix K_{ij} of size $(N - 2) \times (N - 2)$ results from convolution of the curvature tensor \mathbf{R} at the analyzed point on the manifold, $K_{ij} = \langle \mathbf{R}(\mathbf{p}^{(0)}, \mathbf{p}^{(j)}), \mathbf{p}^{(i)} \rangle$.

Let \mathbf{r} be an arbitrary unit vector orthogonal to a vector $\mathbf{p}^{(0)}$ (directed along the geodesic). Then the value of the quadratic form $\sum K_{ij} r_i r_j$ is the curvature of the manifold at the point A in a two-dimensional direction, defined by the vectors $\mathbf{p}^{(0)}$ and \mathbf{r} , which is called the sectional curvature. In particular, in the framework of the construction carried out, the matrix element K_{11} corresponds to the sectional curvature in the direction given by the velocity vector and the first Lyapunov vector (associated with the largest Lyapunov exponent), and the remaining diagonal elements correspond to the curvatures in the directions given by the velocity vector and the other Lyapunov vectors.

Having coefficients $c_i^{(k)}$ related to time points $t - \Delta t$, t , $t + \Delta t$ and taking into account that $c_i^{(k)}(t) = \delta_{ik}$, one can use difference approximation for the second derivative in (20) and obtain the elements of the matrix K_{ij} at A numerically:

$$K_{ij}(t) = \frac{c_i^{(j)}(t - \Delta t) - 2c_i^{(j)}(t) + c_i^{(j)}(t + \Delta t)}{\Delta t^2}. \quad (21)$$

In the case when the system of three rotators is considered, instead of the matrix, we have a single value $K = K_{11}$, which is a function of angular variables and represents the Gaussian curvature of the two-dimensional manifold that is

the Schwarz surface, given by the equation $\cos \theta_0 + \cos \theta_1 + \cos \theta_2 = 0$. This curvature is expressed explicitly [9, 10, 11]:

$$K = -\frac{\cos^2 \theta_0 + \cos^2 \theta_1 + \cos^2 \theta_2}{2(\sin^2 \theta_0 + \sin^2 \theta_1 + \sin^2 \theta_2)^2}. \quad (22)$$

With the analytical formula it is possible to test reliably the above described algorithm by direct comparison of the numerical results and the curvature values from (22). The correspondence turns out to be very good, for example, when specifying the integration step of the fourth-order Runge – Kutta method as $\Delta t = 0.01$, a coincidence occurs up to the fifth significant digit.

Analysis of the formula (22) shows that the curvature is negative over the entire surface with exception of eight points $\theta_0 = \pm\pi/2$, $\theta_1 = \pm\pi/2$, $\theta_2 = \pm\pi/2$, where it is zero because of vanishing of all three cosines. The geodesic flow turns out to belong to the class of Anosov systems, realizing hyperbolic chaos in its conservative version. The presence of points where the curvature is zero does not prevent this, since there are only a finite number of them in the considered compact part of the manifold (the range of variation of the angles from $-\pi$ to π).

Fig. 4a shows a histogram of curvature values at points of a typical trajectory obtained from processing the data of numerical integration of the equations of motion over a sufficiently large time interval. From the histogram it can be seen that the curvature values are distributed in the range from -1 to 0 , which is in accordance with formula (22).

In the case of four rotators, the geodesic flow takes place on a three-dimensional manifold. The matrix K_{ij} has a size 2×2 . Figure 4b shows a histogram of the values of the matrix element K_{11} , which characterizes the sectional curvature of the manifold in the direction given by the velocity vector and the Lyapunov vector corresponding to the largest Lyapunov exponent. Fig. 4c shows the histogram for the K_{22} element that is for the sectional curvature in the direction given by the velocity vector and the second Lyapunov vector, which also corresponds to a positive, but smaller Lyapunov exponent. As can be seen from both histograms, the curvatures for the most part is negative, in which one can find out a correspondence with the chaotic nature of the dynamics; however, positive curvature values also occur with notable statistical significance.

In the case of five rotators, the motion is carried out on a four-dimensional curved manifold, and the matrix K_{ij} has a size 3×3 . Figures 4d, e, f show the histograms of the matrix elements K_{11} , K_{22} , K_{33} , which characterize the sectional curvature of the manifold in the directions specified by the velocity vector and Lyapunov vectors, corresponding to three positive Lyapunov exponents, namely, the largest, the next largest and the smallest one. Again, it can be seen that the curvature is mostly negative, but its positive values are also observed.

The fact of observation of positive values of sectional curvatures in the last two cases $N=4$ and 5 does not necessarily indicate violation of hyperbolicity with certainty, but closes the opportunity to use directly the Anosov theorem concerning everywhere negative sectional curvature to justify it.

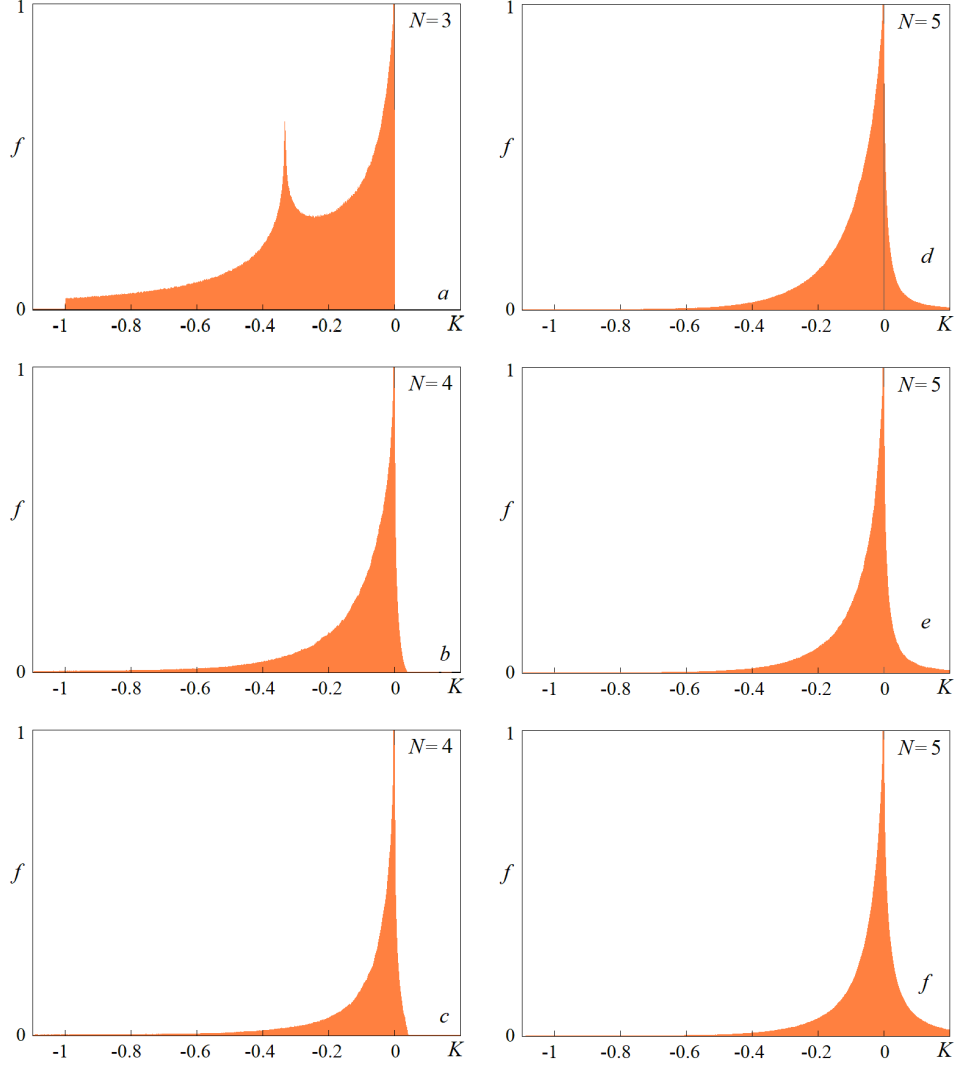


Figure 4: Histograms of curvatures obtained from processing the data of numerical integration of the equations of motion on a typical trajectory for systems composed of $N=3$ (a), $N=4$ (b,c) and $N=5$ (d,e,f) rotators. The histograms (a), (b), (d) correspond to the sectional curvatures in the two-dimensional directions given by the velocity vector and the Lyapunov vector associated with the largest Lyapunov exponent. The remaining histograms for $N=4$ and 5 refer to the sectional curvatures in the directions given by the velocity vectors with the second (c and e) and the third (f) Lyapunov vectors.

4 Angles between subspaces of perturbation vectors

The idea of testing hyperbolicity based on evaluating angles between stable and unstable directions for saddle invariant sets was proposed in [28] and after that it was applied to various situations of chaotic dynamics in a number of specific examples of dynamical systems [29, 30, 31]. The technique consists in the following. A typical trajectory belonging to the invariant set under consideration is traversed forth in time and then back in time, and at the visited points the angles between the subspaces of vectors of small perturbations are determined and their statistical distribution is analyzed. If the distribution obtained does not contain angles close to zero, this indicates the hyperbolicity of the invariant set. Contrary, if a positive probability of zero angles is detected, then tangencies between the stable and unstable subspaces occur, and there is no hyperbolicity.

In the case of high-dimensional systems, to identify a contracting subspace it is more convenient to use not vectors belonging to it, but vectors defining its orthogonal complement, whose dimension is usually small [32]. The latter are obtained from solution of the adjoint system of linearized equations in variations [32, 33, 34, 35].

We start with calculating the reference orbit $\mathbf{x}(t)$ integrating the equations of motion (8), which we write symbolically here as $\dot{\mathbf{x}} = \mathbf{F}(\mathbf{x}, t)$, for a sufficiently large time interval. Then we take the linearized equations for the perturbation vectors $\dot{\tilde{\mathbf{x}}} = \mathbf{F}'(\mathbf{x}(t), t)\tilde{\mathbf{x}}$ (equation (17)), in a number equal to the dimension of the unstable subspace of interest m , and integrate it along the reference trajectory $\mathbf{x}(t)$ with orthogonalization and normalization of the vectors at each step.¹ Next, we carry out integration in reverse time, along the same reference trajectory, for a set of m equations $\dot{\mathbf{u}} = -[\mathbf{F}'(\mathbf{x}(t), t)]^T \mathbf{u}$, where the superscript T means the matrix conjugation. This gives a set of vectors defining an orthogonal complement to the subspace of perturbations with zero and negative Lyapunov exponents. The resulting vectors are also orthogonalized and normalized. On the basis of these data, the angles between the subspaces of the dimension of interest are estimated at the points of the trajectory at each step. (The angle between two subspaces is defined as the minimal possible angle between two vectors, one of which belongs to one and the other to another subspace.)

Figure 5a shows the numerically obtained histogram of the distribution of angles between a one-dimensional unstable subspace and a subspace formed by vectors with negative and zero Lyapunov exponents, at points of a typical trajectory for a system of three rotators with a unit velocity along the geodesic. As seen, the distribution is obviously distant from zero values of the angles ϕ , that is, the test confirms the hyperbolicity of the geodesic flow.

Figures 5b and 5c show the results of testing hyperbolicity for systems of

¹The scalar product is defined here in the full tangent space of dimension $2N$, as the sum of the products of the coordinate and velocity components of the perturbation vectors, in contrast to the previous two sections. Note that the values of the Lyapunov exponents do not depend on the choice of one or the other definition of the scalar product.

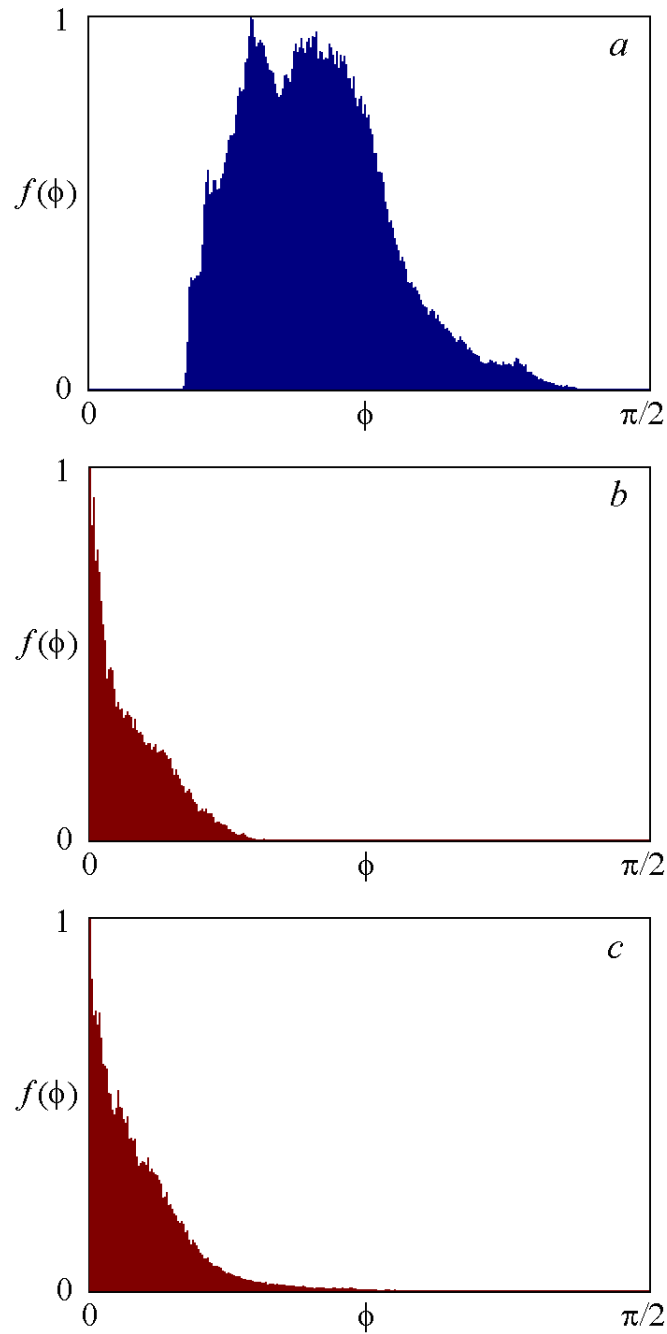


Figure 5: Histograms for angles between unstable subspaces of perturbation vectors of a typical trajectory and subspaces corresponding to vectors with negative and zero Lyapunov exponents, obtained from processing data of numerical calculations for systems based on $N=3$ (*a*), $N=4$ (*b*) and $N=5$ (*c*) rotators.

four and five rotators. Here are histograms of the distributions of angles between unstable subspaces, having a dimension, respectively, two and three, and subspaces of vectors with negative and zero Lyapunov exponents for the case of motion along the geodesics with unit velocity in these systems. Observe that the histograms show definitely an occurrence of angles close to zero, which indicates the presence of tangencies of stable and unstable subspaces and the non-hyperbolic nature of the geodesic flow.

5 Conclusion

The starting point of this work was the remarkable result of Hunt and MacKay [9], who pointed out the Thurston and Weeks triple linkage mechanism [8] as an example of physically realizable mechanical system providing Anosov's chaotic dynamics for a geodesic flow on a two-dimensional curved manifold. The same type of dynamics takes place for a simplified version of the system, where the condition of mechanical constraint on the elements constituting the system has the form of vanishing the sum of the cosines of the rotation angles [13, 14]. The question was whether the dynamics of systems built by this sample with a greater number of elements would have similar properties. In the present work, I give a negative answer, at least for the models where the constraint condition is written as equality to zero of the sum of the cosines for the revolution angles of the rotators.

Namely, numerical calculations show that for the number of elements four and five, when the dynamics correspond to geodesic flows on three-dimensional and four-dimensional manifolds, the conditions of negative sectional curvature, which would be sufficient for realization of the Anosov dynamics, do not hold. Also, on the basis of numerical calculations, it was found that for systems of four and five elements, the hyperbolicity condition requiring the transversality of the intersection of subspaces associated with positive Lyapunov exponents and with non-positive exponents is not satisfied. These results contrast with the case of three rotators corresponding to the geodesic flow on a two-dimensional manifold, the Schwarz surface, where the calculations carried out using the same algorithms confirm belonging to the class of Anosov systems and the hyperbolicity condition is satisfied in the sense of the absence of tangencies between the subspaces of the perturbation vectors.

Nevertheless, the dynamics in all the considered cases is chaotic, as evidenced by the observed waveforms, calculations of Lyapunov exponents, and power spectra of the motions generated by the systems.

For a system of three elements, an approach was previously developed that allows one to arrange the Anosov dynamics on attractor in a system that is an electronic analog, a chaos generator with spectral characteristics satisfactory from the point of view of radiophysical applications [13, 14, 15]. Similarly, it is possible to implement electronic analogs for the systems composed of four, five or more elements, which will generate hyperchaos, the chaotic dynamics with two or more positive Lyapunov exponents.

Returning to the mechanical systems in the form of rotators with constraints determined by algebraic equations, it can be noted that the question of a possible occurrence of Anosov's dynamics for geodesic flows on manifolds of dimension three and higher in such systems cannot be considered completely closed. For example, a possibility remains unexplored of using various distributions of masses among the elements constituting the system.

This work was supported by Grant no. 15-12-20035 of the Russian Science Foundation. The author thanks P.V. Kuptsov for help in calculating the angles between the subspaces of the perturbation vectors, the results of which are presented in Section 4.

Appendix

The flat linkage shown in Fig. 1b can be interpreted as four rotators that revolve around axes located at the vertices of a square with coordinates $(\pm 1, 0)$ and $(0, \pm 1)$. The imposed constraint is due to the connection of the rotators by the rods of length R , attached to them by hinges at a distance ε from the axes and also attached to the hinges placed at the vertices of a square on a moving disk, at a distance ρ from its center. Let x and y be coordinates of the center of the disk, and α is the rotation angle of the disk. The rotation angles of the rotators are counted from vertical or horizontal coordinate axes, as shown in the figure, so that the coordinates of the end joints are

$$(1 - \varepsilon \cos \theta_0, \varepsilon \sin \theta_0), (\varepsilon \sin \theta_1, 1 + \varepsilon \cos \theta_1), \\ (-1 + \varepsilon \cos \theta_2, -\varepsilon \sin \theta_2), (-\varepsilon \sin \theta_3, -1 - \varepsilon \cos \theta_3).$$

The coordinates of the four hinges located on the disk are

$$(x + \rho \cos \alpha, y + \rho \sin \alpha), (x - \rho \sin \alpha, y + \rho \cos \alpha), \\ (x - \rho \cos \alpha, y - \rho \sin \alpha), (x + \rho \sin \alpha, y - \rho \cos \alpha).$$

An instantaneous configuration of the system is given by the angular variables $\theta_0, \theta_1, \theta_2, \theta_3$, of which only three are independent due to the imposed mechanical constraint. Thus, the configuration space is a three-dimensional manifold. The equations that define the mechanical constraint are

$$(1 - \varepsilon \cos \theta_0 - x - \rho \cos \alpha)^2 + (\varepsilon \sin \theta_0 - y - \rho \sin \alpha)^2 = R^2, \\ (\varepsilon \sin \theta_1 - x + \rho \sin \alpha)^2 + (1 + \varepsilon \cos \theta_1 - y - \rho \cos \alpha)^2 = R^2, \\ (-1 + \varepsilon \cos \theta_2 - x + \rho \cos \alpha)^2 + (-\varepsilon \sin \theta_2 - y + \rho \sin \alpha)^2 = R^2, \\ (-\varepsilon \sin \theta_3 - x - \rho \sin \alpha)^2 + (-1 - \varepsilon \cos \theta_3 - y + \rho \cos \alpha)^2 = R^2.$$

Let us turn now to consideration of the asymptotic case when $\varepsilon \ll R$, $\rho \sim \varepsilon$, $(x, y) \sim \varepsilon$, and $R=1$. Taking into account the terms of the first order in the Taylor expansions, we have

$$-\varepsilon \cos \theta_0 - x - \rho \cos \alpha = 0, \quad -\varepsilon \cos \theta_1 + y + \rho \cos \alpha = 0, \\ -\varepsilon \cos \theta_2 + x - \rho \cos \alpha = 0, \quad -\varepsilon \cos \theta_3 - y + \rho \cos \alpha = 0.$$

Summating the equations, we get

$$\cos \theta_0 + \cos \theta_1 + \cos \theta_2 + \cos \theta_3 = 0.$$

Assuming that the massive elements of the system are only the rotators, each characterized by a unit moment of inertia, for the kinetic energy we have to write $T = \frac{1}{2}(\dot{\theta}_0^2 + \dot{\theta}_1^2 + \dot{\theta}_2^2 + \dot{\theta}_3^2)$. For our system, this expression is just the Lagrange function. From the conditional extremum of the action functional $\int (T - \Lambda F)dt$ with taking into account the imposed constraint, we obtain finally the equation of motion in the form (7) or (8) for $N=4$.

References

- [1] Paternain G.P. Geodesic Flows. *Progress in Mathematics*, Book 180. Birkhäuser, 1999, 149 p.
- [2] Dubrovin B.A., Fomenko A.T., Novikov S.P. *Modern geometry – methods and applications: Part II: The geometry and topology of manifolds*, Springer Science & Business Media, 2012. 432 p.
- [3] Hadamard J. Les surfaces à courbures opposées et leurs lignes géodésique, *Journal de Mathématiques Pures et Appliquées*, 1898, vol. 4, pp. 27–73.
- [4] Anosov D.V. Roughness of geodesic flows on compact Riemannian manifolds of negative curvature, *Dokl. Akad. Nauk SSSR*, 1962, vol. 145, no. 4, pp. 707–709 (in Russian).
- [5] Anosov D.V. Geodesic flows on closed Riemannian manifolds of negative curvature, *Trudy Matematicheskogo Instituta Imeni VA Steklova*, 1967, vol. 90, pp. 3–210 (in Russian).
- [6] Anosov D.V., Sinai Y.G. Some smooth ergodic systems, *Russian Mathematical Surveys*, 1967, vol. 22, no. 5, pp. 103–167.
- [7] Anosov D.V., Aranson S.Kh., Grines V.Z., Plykin R.V., Sataev E.A., Saponov A.V., Solodov V.V., Starkov A.N., Stepin A.M., and Shlyachkov S.V., *Dynamical Systems with Hyperbolic Behaviour. Dynamical Systems IX*, *Encycl. Math. Sci.*, vol. 66, Berlin: Springer, 1995, 236 p.
- [8] Thurston W.P. and Weeks J.R. The mathematics of three-dimensional Manifolds, *Sci. Am.*, 1984, vol. 251, pp. 94–106.
- [9] Hunt T.J. and MacKay R.S. Anosov parameter values for the triple linkage and a physical system with a uniformly chaotic attractor, *Nonlinearity*, 2003, vol. 16, pp. 1499–1510.
- [10] Kuznetsov S.P. Chaos in the System of Three Coupled Rotators: from Anosov Dynamics to Hyperbolic Attractor, *Izv. Saratov Univ. (N. S.), Ser. Physics*, 2015, vol. 15, issue 2, pp. 15–17 (in Russian).

- [11] Kuznetsov S.P. Hyperbolic Chaos in Self-oscillating Systems Based on Mechanical Triple Linkage: Testing Absence of Tangencies of Stable and Unstable Manifolds for Phase Trajectories, *Regular and Chaotic Dynamics*, 2015, vol. 20, no. 6, pp. 649–666.
- [12] Meeks W.H. III, Ros A., Rosenberg H. *The Global Theory of Minimal Surfaces in Flat Spaces: Lectures given at the 2nd Session of the Centro Internazionale Matematico Estivo (C.I.M.E.)* (Lecture Notes in Mathematics, Book 1775), Springer, 2002, 124 p.
- [13] Kuznetsov S.P. From Anosov’s Dynamics on a Surface of Negative Curvature to Electronic Generator of Robust Chaos, *Izv. Saratov Univ. (N. S.), Ser. Physics*, 2016, vol. 16, issue 3, pp. 131–144 (in Russian).
- [14] Kuznetsov S.P. From Geodesic Flow on a Surface of Negative Curvature to Electronic Generator of Robust Chaos, *International Journal of Bifurcation and Chaos in Applied Sciences and Engineering*, 2016, vol. 26, no. 14, 1650232, 8 p.
- [15] Kuznetsov S.P. Chaos in three coupled rotators: From Anosov dynamics to hyperbolic attractors, *Indian Academy of Sciences Conference Series*, 2017, vol. 1, no. 1, p. 117–132.
- [16] Felk E.V., Kuznetsov S.P., Savin A.V. Diffusion in the configuration space of a system of two coupled rotators, *Materials of the XI International School-Conference "Chaotic Self-Oscillations and Pattern Formation" (CHAOS-2016)*, Saratov State University, Saratov: Publishing Center "Science", 2016, p.110 (in Russian).
- [17] Zaslavskii G.M., Sagdeev R.Z., Usikov D.A., Chernikov A.A. *Weak Chaos and Quasi-Regular Patterns*, Cambridge Nonlinear Science Series (Book 1), Cambridge University Press, 1991. 268 p.
- [18] Dubrovin B.A., Fomenko A.T., Novikov S.P. *Modern Geometry Methods and Applications: Part I: The Geometry of Surfaces, Transformation Groups, and Fields*, 2nd edition, Springer 1991, 470 p.
- [19] Sveshnikov A.A. *Applied methods of the theory of random functions*, Elsevier, 2014, 332 p.
- [20] Jenkins G.M., Watts D.G. *Spectral analysis and its applications*, Holden-Day, 1969, 525 p.
- [21] Benettin G., Galgani L., Giorgilli A., and Strelcyn J.-M. Lyapunov Characteristic Exponents for Smooth Dynamical Systems and for Hamiltonian Systems: A Method for Computing All of Them, *Meccanica*, 1980, vol. 15, pp. 9–30.

- [22] Shimada I. and Nagashima T. A numerical approach to ergodic problem of dissipative dynamical systems, *Progress of Theoretical Physics* 1979, vol. 61, pp. 1605-1616.
- [23] Kuznetsov S.P. *Hyperbolic Chaos: A Physicist's View*, Beijing: Higher Education Press, and Berlin, Heidelberg: Springer-Verlag, 2012, 336 p.
- [24] Pikovsky A., Politi A. *Lyapunov Exponents: A Tool to Explore Complex Dynamics*, Cambridge University Press, 2016. 295 p.
- [25] Kuptsov P.V. Computation of Lyapunov exponents for spatially extended systems: advantages and limitations of various numerical methods, *Izvestiya VUZ, Applied Nonlinear Dynamics*, 2010, vol. 18, issue 5, pp. 91-110 (in Russian).
- [26] Rössler O.E. An equation for hyperchaos, *Physics Letters A*, 1979, vol. 71, no. 2-3, pp. 155–157.
- [27] Letellier C. and Rössler O.E. Hyperchaos, *Scholarpedia*, 2007, vol. 2, issue 8, p. 1936.
- [28] Lai Y.-Ch., Grebogi C., Yorke J.A., and Kan I. How Often Are Chaotic Saddles Nonhyperbolic?, *Nonlinearity*, 1993, vol. 6, no. 5, pp. 779–798.
- [29] Anishchenko V.S., Kopeikin A.S., Kurths J., Vadivasova T.E., Strelkova G.I. Studying Hyperbolicity in Chaotic Systems, *Phys. Lett. A*, 2000, vol. 270, no. 6, pp. 301–307.
- [30] Kuznetsov S.P. Dynamical chaos and uniformly hyperbolic attractors: from mathematics to physics, *Physics-Uspokhi*, 2011, vol. 54, issue 2, pp. 119–144.
- [31] Kuznetsov S.P., Kruglov V.P. On Some Simple Examples of Mechanical Systems with Hyperbolic Chaos, *Proceedings of the Steklov Institute of Mathematics*, 2017, vol. 297, pp. 208–234.
- [32] Kuptsov P.V., Fast Numerical Test of Hyperbolic Chaos, *Phys. Rev. E*, 2012, vol. 85, no. 1, 015203, 4 p.
- [33] Kuptsov P.V. and Kuznetsov S.P. Numerical test for hyperbolicity of chaotic dynamics in time-delay systems, *Phys. Rev. E*, 2016, vol. 94, no. 1, 010201, 6 p.
- [34] Kuptsov P.V., Kuznetsov S.P. Numerical test for hyperbolicity in chaotic systems with multiple time delays, *Communications in Nonlinear Science and Numerical Simulation*, 2018, vol. 56, pp. 227–239.
- [35] Kuptsov P.V., Kuznetsov S.P. Lyapunov analysis of strange pseudohyperbolic attractors: Angles between tangent subspaces, local volume expansion and contraction, 2018, arXiv: 1805.06644 [nlin.CD].